

## Supporting Information

### Developing antibacterial nanocrystalline cellulose using natural antibacterial agents

Mandana Tavakolian<sup>1,3</sup>, Mira Okshevsky<sup>1,3</sup>, Theo G.M. van de Ven<sup>2,3</sup>, and Nathalie Tufenkji<sup>\*,1,3</sup>

<sup>1</sup>Department of Chemical Engineering, McGill University, Montréal, Québec, Canada H3A 0C5

<sup>2</sup>Department of Chemistry, McGill University, Montréal, Québec, Canada H3A 2K6

<sup>3</sup>Quebec Centre for Advanced Materials, Canada (QCAM/CQMF)

\*Corresponding author email: [nathalie.tufenkji@mcgill.ca](mailto:nathalie.tufenkji@mcgill.ca)

## 1. Reaction schemes:

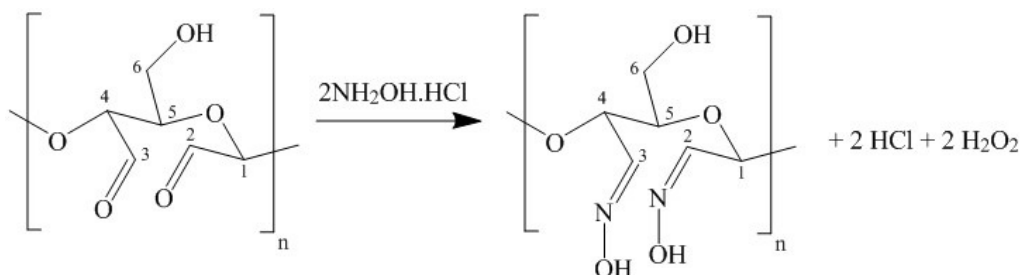


**Figure S1.** The reaction in hydroxylamine-hydrochloride (NH<sub>2</sub>OH.HCl) titration.

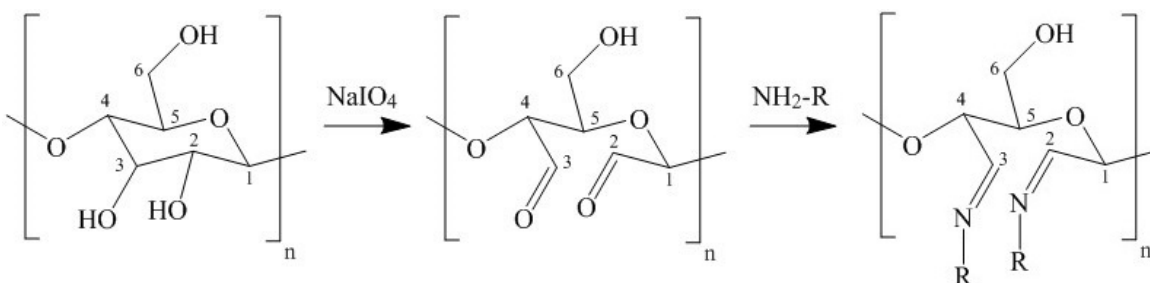
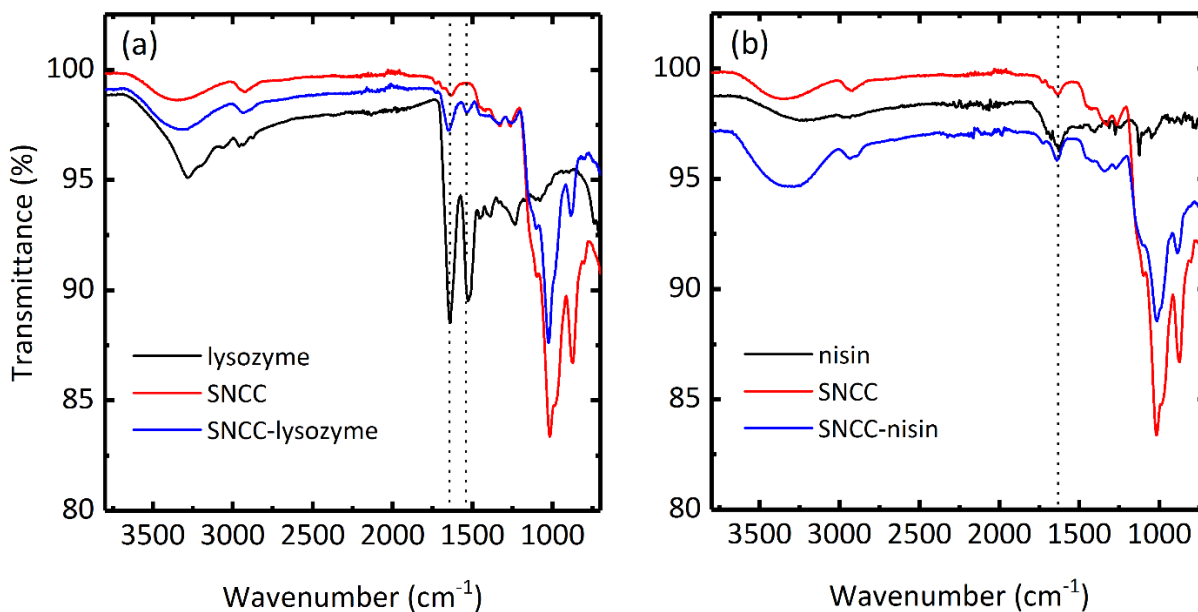


**Figure S2.** Schematic of periodate oxidation of cellulose and Schiff base reactions.

## 2. FTIR Spectroscopy:

We used FTIR spectroscopy to further investigate the attachment of antibacterial agents to SNCC. Figure S3a shows the FTIR spectra of SNCC, lysozyme, and SNCC-lysozyme. For SNCC, the peak at 3340 cm<sup>-1</sup> indicates the stretching of -OH groups, and the peaks at 2900, 1430, and 1030 cm<sup>-1</sup> signify C-H stretching, -CH<sub>2</sub> scissoring and CH<sub>2</sub>-O-CH<sub>2</sub> stretching, respectively.<sup>1</sup> The FTIR spectra of SNCC has two main characteristic peaks. The peaks at 1730 and 880 cm<sup>-1</sup> are indicative of the carbonyl groups stretching and the hemiacetal linkage formed by the dialdehyde groups, respectively.<sup>2</sup> For lysozyme, the peak at 3275 cm<sup>-1</sup> is due to the stretching of the primary amine. The peak at 1650 cm<sup>-1</sup> is due to the C=O stretching mode, whereas the peak at 1543 cm<sup>-1</sup> is due to the bending and the stretching mode of N-H and C-N vibrations, respectively. The peak at 1250

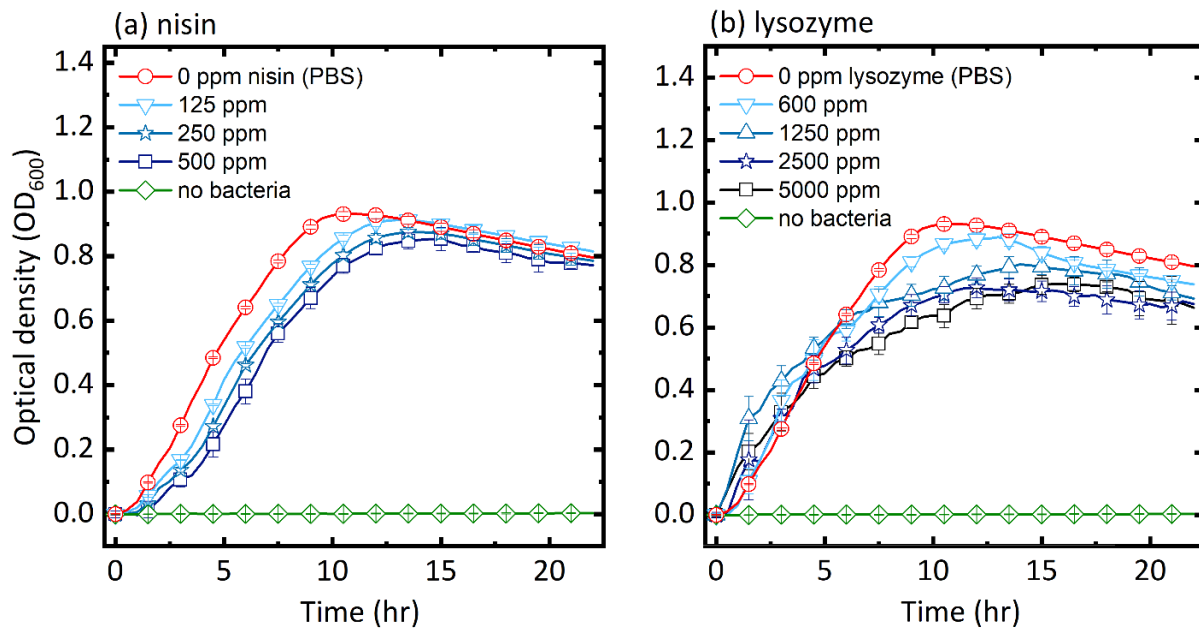
$\text{cm}^{-1}$  is due to the stretching and the bending mode of C–N and N–H vibrations. The bands near  $1453$  and  $1400 \text{ cm}^{-1}$  are ascribed to  $\text{CH}_2$  and  $\text{CH}_3$  stretching modes of the aliphatic moieties of the amino acid side chains.<sup>3-4</sup> The presence of the peaks at  $1650 \text{ cm}^{-1}$  and  $1543 \text{ cm}^{-1}$  in the spectra of SNCC-lysozyme confirm the presence of lysozyme. For nisin, as shown in Figure S3b, the amide I band at  $1650 \text{ cm}^{-1}$  (C=O stretching) increases with the presence of nisin on SNCC which confirms its attachment to SNCC.<sup>5</sup>



**Figure S3.** FTIR spectra of (a) SNCC, lysozyme, and SNCC-lysozyme and (b) SNCC, nisin, and SNCC-nisin. The dashed lines at  $1650 \text{ cm}^{-1}$  and  $1543 \text{ cm}^{-1}$  show the location of C=O stretching and C–N vibration, respectively.

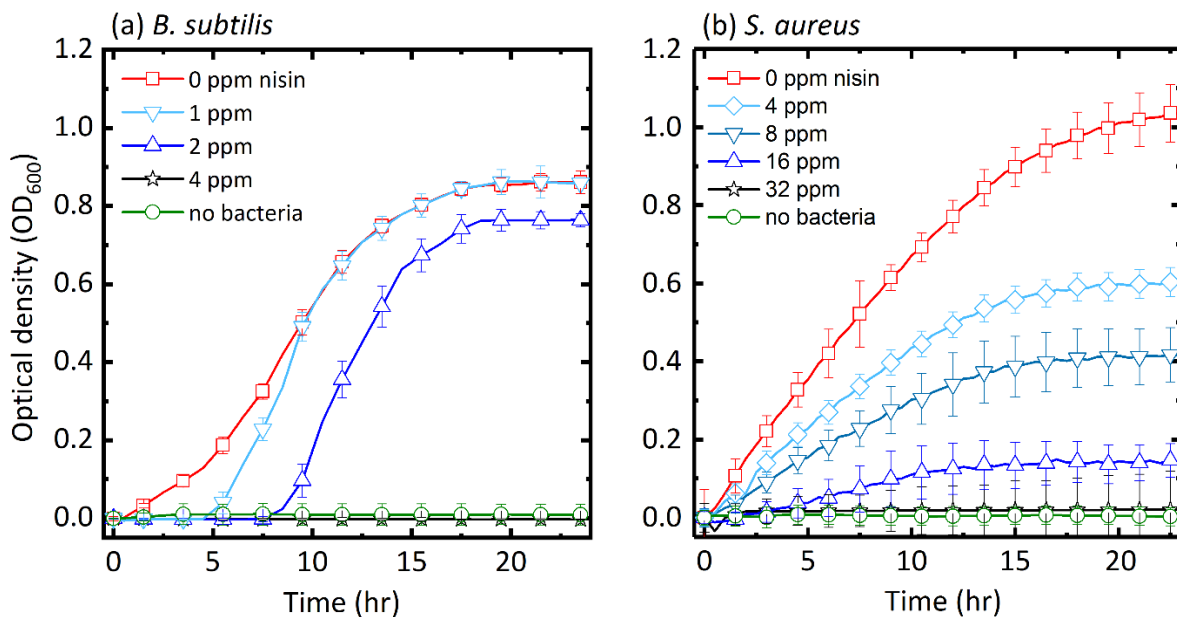
### 3. Antibacterial activity of nisin and lysozyme in free form

Figure 4 shows the growth curve of *E. coli* K12 as a model Gram-negative bacterium exposed to different concentrations of free nisin (Fig. S4a) and free lysozyme (Fig. S4b). It shows that even at very high concentrations of nisin and lysozyme, they are not effective against Gram-negative bacteria.



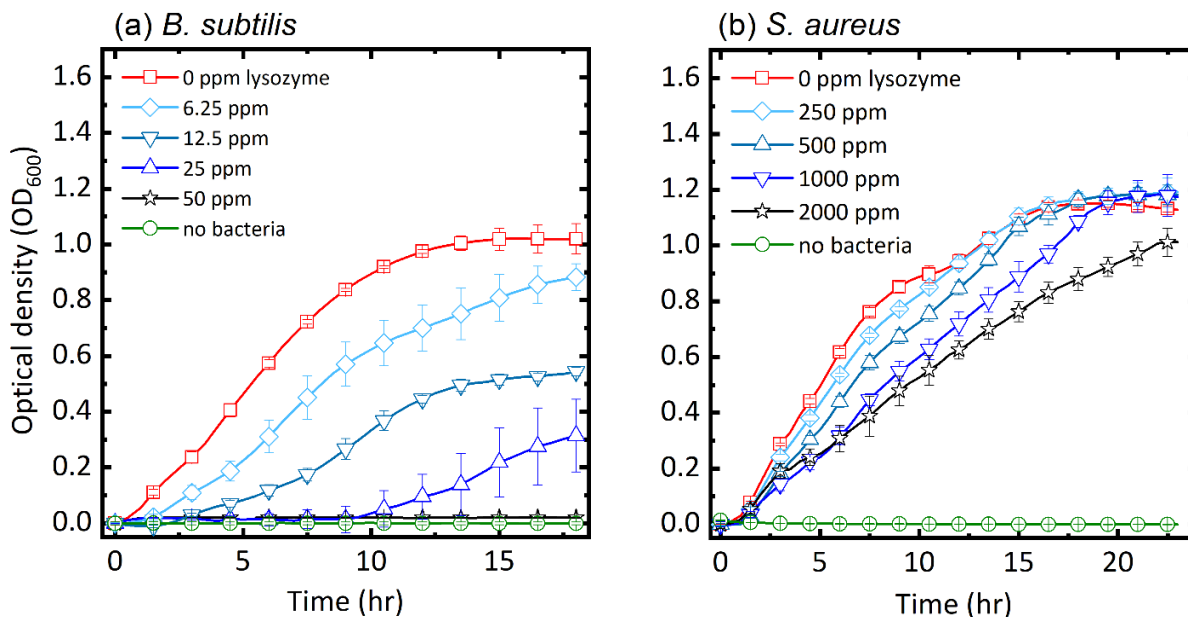
**Figure S4.** Growth curves of *E. coli* exposed to different concentrations of (a) nisin and (b) lysozyme.

Figure S5a shows the growth curves of *B. subtilis* exposed to different concentrations of nisin. The MIC of nisin for *B. subtilis* was measured to be approximately 4 ppm. Nisin was also tested against *S. aureus* ATCC 25923. The MIC of nisin for *S. aureus* was measured to be 32 ppm (Fig. S5b).



**Figure S5.** Growth curves of (a) *B. subtilis* and (b) *S. aureus* in the presence of different concentrations of nisin.

Lysozyme was tested against *B. subtilis* with concentrations of 6.25, 12.5, 25, and 50 ppm in PBS. Lysozyme was also tested against *S. aureus* with much higher concentrations up to 2000 ppm. A suspension of bacteria and PBS, and a suspension of LB and PBS were used as controls to ensure maximum growth and no growth, respectively. The OD<sub>600</sub> of the samples were measured overnight and the MIC of lysozyme was measured to be about 50 ppm (Fig. S6).



**Figure S6.** Growth curves of (a) *B. subtilis* and (b) *S. aureus* in the presence of different concentrations of lysozyme.

## References

- (1) Keshk, S. M. Homogenous Reactions of Cellulose from Different Natural Sources. *Carbohydrate Polymers* **2008**, *74* (4), 942-945.
- (2) Kim, U.-J.; Wada, M.; Kuga, S. Solubilization of Dialdehyde Cellulose by Hot Water. *Carbohydrate Polymers* **2004**, *56* (1), 7-10.
- (3) de Oliveira, L. F.; de Almeida Gonçalves, K.; Boreli, F. H.; Kobarg, J.; Cardoso, M. B. Mechanism of Interaction between Colloids and Bacteria as Evidenced by Tailored Silica–Lysozyme Composites. *Journal of Materials Chemistry* **2012**, *22* (43), 22851-22858.
- (4) Byler, D. M.; Susi, H. Examination of the Secondary Structure of Proteins by Deconvolved Ftir Spectra. *Biopolymers* **1986**, *25* (3), 469-487.
- (5) Qi, X.; Poernomo, G.; Wang, K.; Chen, Y.; Chan-Park, M. B.; Xu, R.; Chang, M. W. Covalent Immobilization of Nisin on Multi-Walled Carbon Nanotubes: Superior Antimicrobial and Anti-Biofilm Properties. *Nanoscale* **2011**, *3* (4), 1874-1880.